

Localized vibrational modes in GaN:O tracing the formation of oxygen *DX*-like centers under hydrostatic pressure

C. Wetzel*

High Tech Research Center, Meijo University, 1-501 Shiogamaguchi, Tempaku-ku, Nagoya 468-8502, Japan

H. Amano and I. Akasaki

High Tech Research Center and Department of Electrical and Electronic Engineering, Meijo University, 1-501 Shiogamaguchi, Tempaku-ku, Nagoya 468-8502, Japan

J. W. Ager III

Materials Sciences Division, Lawrence Berkeley National Laboratory, Berkeley, California 94720

I. Grzegory

UNIPRESS High Pressure Research Center, Polish Academy of Sciences, Sokolowska 29/37, 01-142 Warszawa, Poland

M. Topf and B. K. Meyer

1. Physikalisches Institut, Justus-Liebig-Universität Giessen, 35392 Giessen, Germany

(Received 22 October 1999)

Vibrational modes are observed at ambient pressure in O-doped GaN at 544 cm^{-1} using Raman spectroscopy. Investigation of these modes with applied hydrostatic pressure reveals the existence of three closely spaced modes that shift in relative intensity with increasing pressure. Notably, transitions between the different modes occur at previously observed electronic transitions associated with the *DX*-like center behavior of substitutional O on the N site. A simple one-dimensional oscillator model is used to extract approximate force constants; these are consistent with the assignment of the 544 cm^{-1} mode to O_N and with force constants for C and B dopants in GaP. The relative intensity changes observed at 11 and 17 GPa are assigned to changes in the charge state due to the merging of the $+/0$ ionization level and the Fermi energy and the transition to DX^- that causes a previously observed drop in free electron concentration, respectively.

I. INTRODUCTION

The practical development of GaN for application in optoelectronic, high frequency, high power, and high temperature devices^{1,2} is closely linked to the control of defects and impurities. The development of suitable buffer layer techniques, precursor purification, and successful acceptor activation are essential steps in the development of working devices.³ An important step in the identification of impurities was the recent clarification of the role of O.⁴⁻⁶ In contrast to its behavior in Ge, Si, GaAs, and GaP, O is a highly effective shallow donor in GaN and, due to this unexpected behavior, it is a major source of high background *n*-type conductivity. For example, in vapor phase epitaxy O can be incorporated at high concentrations by water contamination of the ammonia precursor. Oxygen also poses a problem during growth in the high vacuum systems used in molecular beam epitaxy.

A convenient and important tool for elemental impurity analysis is the study of their vibrational modes in infrared absorption or in Raman spectroscopy.⁷ However, no vibrational modes of donors have so far been identified in GaN. The electronic properties of GaN:O reveal a *DX*-like behavior of O under large hydrostatic pressure.^{4,8,9} In Raman spectroscopy we have observed previously a freeze-out of electrons to the deep gap state at pressures above 20 GPa. Oxygen has also been reported as a deep donor in irradiated GaN.¹⁰ Here we report the observation of vibrational modes

in GaN at frequencies where substitutional O is expected and correlate their behavior under hydrostatic pressure with the electronic properties.

II. EXPERIMENTAL PROCEDURE

Epitaxial samples of GaN:O were grown by hydride vapor phase epitaxy (HVPE) on *c*-plane sapphire at thicknesses of $20\text{ }\mu\text{m}$.¹¹ Oxygen doping was achieved by water vapor introduction. Small bulk samples were grown by high pressure/high temperature synthesis.¹² In both cases O concentrations in the range of 10^{18} cm^{-3} to 10^{20} cm^{-3} were measured by secondary ion mass spectroscopy (SIMS) depth profiles. Details of the samples are collected in Table I. Nonresonant Raman spectroscopy was performed using 100 mW of the 476.5 nm line of an Ar ion laser. Large hydrostatic pressure up to $p = 38\text{ GPa}$ was applied by means of a Mao-Bell-type diamond anvil cell using nitrogen as a pressure medium and the luminescence of ruby chips as a scale for pressure and its homogeneity. All data were taken at room temperature.

III. RESULTS

Representative Raman spectra for GaN:O (high carrier concentration *N*) and GaN (low *N*) in two geometries at ambient pressure are shown in Fig. 1. According to the selection rules in wurtzite $A_1(\text{LO})$ and E_2 (high and low) are allowed

TABLE I. Parameters of the GaN samples studied. N_D denotes the averaged experimental impurity concentration of known donor-type species from SIMS profiles.

Sample	Growth	μ_{el} (Hall) ($\text{cm}^2/\text{V s}$)	N_{el} (Hall) (10^{16} cm^{-3})	N_D (SIMS) (10^{16} cm^{-3})
GaN:O	HVPE ^a	90	3500	O:2000, Si:30
Bulk	HPS ^{b,c}	60	1000–5000	O:10000, Si:10

^aSee Ref. 11.

^bHigh pressure synthesis, see Ref. 12.

^cSee Ref. 24.

in the $z(x, -)\bar{z}$ as well as in the $z(x, -)z$ forward scattering geometry.¹³ In scattering along $y(x, -)\bar{y}$, typically obtained from the thin edge of the sample, E_2 , $A_1(\text{TO})$, and $E_1(\text{TO})$ are allowed. In the experiment $E_1(\text{TO})$ appears at $\bar{\nu}(E_1, \text{TO}, p \approx 0) = 559 \text{ cm}^{-1}$ in $y(x, -)\bar{y}$ geometry. $E_2(\text{high})$ appears at $\bar{\nu}(E_2, p \approx 0) = 567 \text{ cm}^{-1}$ in $z(x, -)\bar{z}$ and $y(x, -)\bar{y}$ and a strong mode appears at 531 cm^{-1} in $z(x, -)\bar{z}$ scattering. Although not expected in this geometry this mode must be attributed to $A_1(\text{TO})$ and possible contributions of the lower branch of the $A_1(\text{LO})$ phonon-plasmon coupled mode [here jointly labeled with $A_1(\text{TO})$]. In addition we observe a mode Q at $\bar{\nu} = 544 \text{ cm}^{-1}$ at ambient pressure, which is not expected in the phonon spectrum. In our experiments Q only appears in $z(x, -)z$ or $z(x, -)\bar{z}$ scattering, but not in $y(x, -)y$. We observe Q only in O doped material. We did not observe Q in Si doped material.¹⁴ Reports of phonon quasimodes in the range between $E_1(\text{TO})$ and $A_1(\text{TO})$ modes reveal¹⁵ that such a mode would appear instead of but not in parallel with the TO modes and that it should be broader than either of the TO modes.¹⁶ In addition, the high crystalline quality of bulk crystals from high pressure synthesis makes structural defects unlikely as the cause of Q .

Under hydrostatic pressure (Fig. 2) the phonon modes shift to higher frequencies at slopes of $3.75 \text{ cm}^{-1}/\text{GPa}$ (E_2) and $3.1 \text{ cm}^{-1}/\text{GPa}$ [$A_1(\text{TO})$] in agreement with the

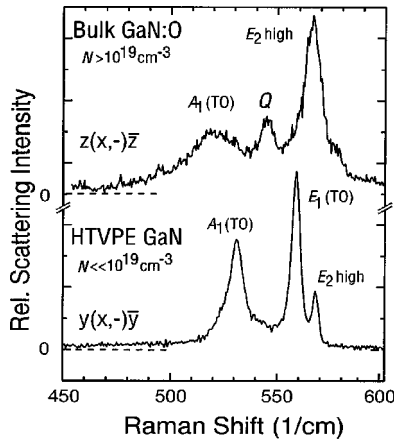


FIG. 1. Raman spectra in the phonon range of GaN in two scattering orientations. $E_1(\text{TO})$ and $E_2(\text{high})$ form a narrow optical phonon band. In GaN:O an additional mode Q appears in $z(x, -)\bar{z}$ scattering below the band of E_1 and E_2 .

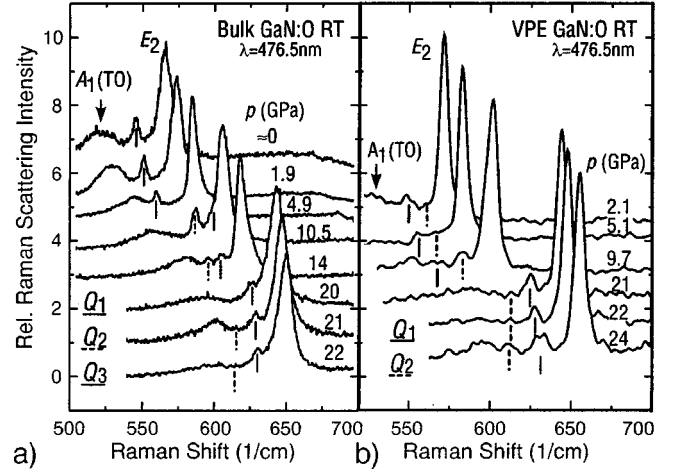


FIG. 2. Raman spectra under variable hydrostatic pressure in bulk (a) and vapor phase (b) GaN:O. In addition to a pressure stiffening of phonon modes Q appears with variable localization energy and under some pressure conditions it appears as set of Q_1 , Q_2 , and Q_3 .

literature.¹² We subsequently use the slope of E_2 as a secondary pressure standard. At certain pressure ranges Q appears as a set of multiple lines Q_1 , Q_2 , and Q_3 with variable intensities. Mode frequencies of several samples versus pressure are collected in Fig. 3. By its definition as the pressure scale the energy of E_2 appears as a straight line. Modes Q_{1-3} have a somewhat smaller pressure dependence, $\approx 2.7 \text{ cm}^{-1}/\text{GPa}$.

For a more detailed analysis of Q we remove the first order pressure dependence of the measured mode energies by scaling all vibrational energies to the frequency of the $E_2(\text{high})$ phonon mode. We next consider the localization energy of Q , $\bar{\nu}_{loc}$, with respect to the lower edge of the optical phonon band represented in this energy range by $E_1(\text{TO})$:

$$\bar{\nu}_{loc} = \bar{\nu}(E_1, \text{TO}, p=0) - \frac{\bar{\nu}(Q_{1-3}, p)}{\bar{\nu}(E_2, p)}. \quad (1)$$

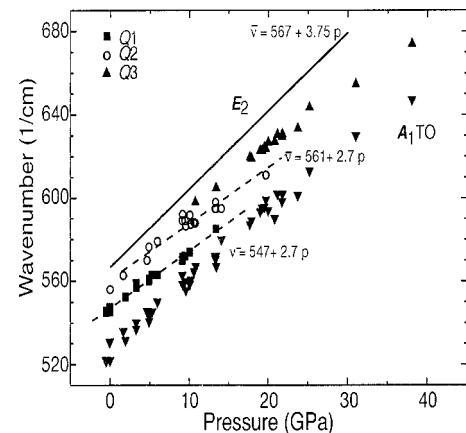


FIG. 3. Phonon and Q mode energies as a function of pressure up to 38 GPa. A significantly different behavior is observed for phonon mode E_2 and Q_{1-3} .

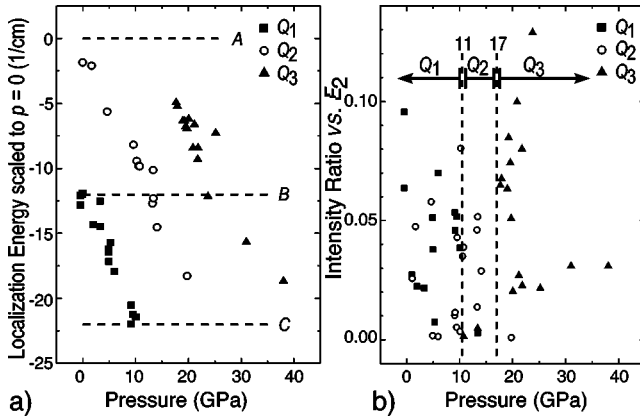


FIG. 4. Q modes versus pressure. (a) Mode energies in units of localization energy with respect to the optical phonon band edge in $E_1(\text{TO})$ in units of ambient pressure. Three descriptive threshold levels A, B, and C are indicated. (b) Intensities of modes Q_{1-3} . Three pressure regimes of respective dominance appear.

The values of $\bar{\nu}_{loc}$ are collected in Fig. 4(a) and the integrated intensities of Q_{1-3} with respect to E_2 are shown in Fig. 4(b). The localization energies together with the relative intensities show a clear grouping of Q into pressure ranges where one of the Q modes is dominant. While Q_1 is the strongest mode for $p < 11$ GPa, Q_2 is dominant in the range $11 \text{ GPa} < p < 17$ GPa and Q_3 is strongest for $p > 17$ GPa. This indicates a sequence of level switchings from Q_1 to Q_2 and then to Q_3 . In this way Q appears at a localization energy of $B = -12 \text{ cm}^{-1}$ at $p \approx 0$ (with respect to a level of $A = 0 \text{ cm}^{-1}$). This (negative) value then increases to a level of $C = -22 \text{ cm}^{-1}$ at $p = 11$ GPa. Then Q switches back to B to follow a weaker line that last can be observed at 17 GPa at some -18 cm^{-1} before the mode switches back again to follow the emerging mode Q_3 up to -19 cm^{-1} at the largest pressures applied here, $p = 38$ GPa.

IV. DISCUSSION

The correlation of the Q modes and the high O concentration suggests they are vibrational modes of O donors substituting on the N site in GaN. We show that such an assumption is reasonable by considering first an isotopical impurity of defect mass $m_O = 16$ amu and in a second step consider variations of the force constants to account for the Coulombic effects of the donor impurity. For this purpose we simulate the lattice vibrations E_1 and E_2 within the basal plane of GaN in a linear chain model considering nearest neighbor interaction in a harmonic mass-and-spring model^{17,18} along $(10\bar{1}0)$. To reflect the hexagonal symmetry we introduce a set of two spring constants k_1 and k_2 which corresponds to an additional zone folding. In this way both maxima [$E_2(\text{high}), E_2(\text{low})$] and minima ($E_1, 0$) of the optical and acoustical phonon bands are zone center phonons. Scaling the eigenvalues to the phonon energies $E_2(\text{low})(144 \text{ cm}^{-1})$ and $E_2(\text{high})(570 \text{ cm}^{-1})$ results in $k_1 = 200.5 \text{ N/m}$ and $k_2 = 26.9 \text{ N/m}$. The respective projections of the bond angles to the high symmetry direction $(10\bar{1}0)$ lead to the large difference between k_1 and k_2 . The model yields $\bar{\nu}(E_1) = 552 \text{ cm}^{-1}$ which coincides well with $E_1(\text{TO})$

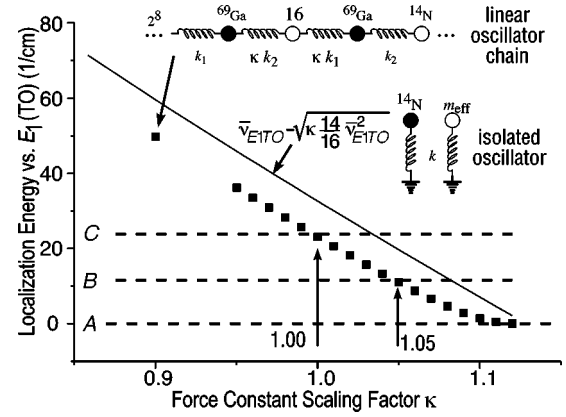


FIG. 5. Localization energies of a Coulombic oscillator of mass 16 amu substituting for N in GaN with variable force constant κ . The solid line holds for an isolated harmonic oscillator and the filled squares for the linear chain model with two force constants. The experimental switching levels A, B, and C are indicated.

and supports the suitability of this model. By substituting a N atom with O a zone center mode associated with the O atom appears at $\bar{\nu}_O = \bar{\nu}(E_1) - 23 \text{ cm}^{-1} = 529 \text{ cm}^{-1}$ in this framework. The associated amplitude is ten times as large as that of the E_1 mode in the unperturbed system. At the same time the amplitudes of E_1 and $E_2(\text{high})$ modes are reduced by about a factor of ten, resulting altogether in a large expected signal amplitude of the O mode with respect to the optical phonon band. Further details of the calculation are given elsewhere.¹⁶ The small deviation of the Q -mode frequencies and the expected value for O_N , $\Delta\bar{\nu} = 15 \text{ cm}^{-1}$, support our assignment of Q to vibrational modes of substitutional O.

In order to account for the remaining discrepancy between the calculated and observed vibrational frequencies, we next consider variations of the effective force constants by introducing a scaling factor κ to the pair of k_1 and k_2 next to the impurity atom. The results of varying κ to reproduce our observed frequencies are shown in Fig. 5 together with the threshold levels A, B, and C. The case of decoupled oscillators ($m_{\text{Ga}} \rightarrow \infty$) is also shown (solid line). Within the model of coupled oscillators (filled squares), the switching sequence of the Q_{1-3} modes appears as follows. Starting at level B ($\kappa = 1.05$), Q moves to C and κ falls to $\kappa = 1.00$ before with increasing pressure it switches back to B and $\kappa = 1.05$. It then moves up toward C again. In parallel to this behavior of the dominant mode, modes Q_2 and Q_3 coexist. They first appear at or near level A ($\kappa = 1.11$) and move to B and C, respectively, before they receive major intensity. This variation of 5% in the force constants compares reasonably well with the relative change of the nuclear charge from N to O (14%) and the calculated bond length variation around the O impurity, 3–4.2%.^{19,20} Within this limited model of a Coulombic defect oscillator the continuous variation of the localization energy could produce a variation of the force constants due to the screening conditions of the defect. The steps from Q_1 to Q_2 and Q_2 to Q_3 of $\Delta\kappa \approx 0.05$ can then be explained as different charge states of the defect. Such a variation of the vibrational mode energy with the charge state has also been seen for Si in InP.²¹

The switching from Q_2 to Q_3 at 17 GPa occurs close to the previously observed onset of carrier freeze-out to the

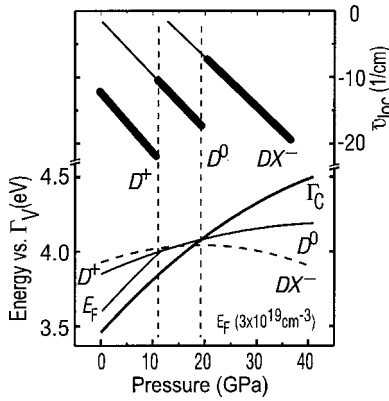


FIG. 6. Model of the pressure dependence of band gap, Fermi energy, and different charge states of the O DX -like donor states in GaN. The steps in Q closely correspond to the crossings of the donor levels with the Fermi edge and the conduction band edge, respectively.

DX -like center of O at 20 ± 2 GPa.⁴ This also agrees with the threshold seen in infrared absorption.²² This 0/- charging step leads to the DX^- state, which according to first principles calculations is accompanied by a large lattice relaxation around the O impurity.⁵ Based on the experimental localization energy of the electronic donor level at 27 GPa and band structure calculations, we previously⁸ developed a model (Fig. 6) for the pressure dependence of the electronic conduction band and the +/0 ionization level of the strongly localized donor. The pressure dependence of DX^- is a spline interpolation to theoretical values of the correlation energy.⁵ Within the same picture the switching from Q_1 to Q_2 at 11 GPa can be associated with the merging of the +/0 ionization level and the Fermi energy for a carrier concentration $N = 3 \times 10^{19} \text{ cm}^{-3}$.

Based on this close correspondence between the electronic charging regimes of O and the vibrational modes, Q_1 can be associated with a vibration of the electronic D^+ state, while Q_2 would correspond to the neutral D^0 state after trapping electrons from the Fermi sea. Such a level has so far not been found in theory.⁵ Q_3 would correspond to the DX^- state. The different vibration modes therefore show a close correspondence with the expected trapping dynamics of the DX -like center of the O donor. All the observed vibrations are associated with the in-basal plane modes while the large lattice relaxation of O is calculated to move perpendicular to this plane. Due to the uniaxial nature of the lattice the local defect symmetry is well aligned with and replicates the crystal orientation. In extrapolation to ambient pressure we expect the vibration modes at 547 cm^{-1} (Q_1), 561 cm^{-1} (Q_2), and 565 cm^{-1} (Q_3). The first two share a

similar pressure behavior, while the latter two are in resonance with the optical phonon band between $E_1(\text{TO})$ and $E_2(\text{high})$ at ambient pressure.

Vibrational modes of substitutional group-VI $^{32}\text{S}_\text{P}^+$ donors in GaP have been identified at 272.5 cm^{-1} .²³ The associated ratio of the force constants corresponds to $\kappa = 0.49$ and indicates a significantly different case. On the other hand, vibrational gap modes of lighter substitutional impurities on the zinc blende GaP group-V site yield values of $\kappa \approx 1$. As Newman⁷ pointed out the squares of the vibrational modes of ^{10}B , ^{11}B , ^{12}C , ^{13}C , and ^{14}C in GaP follow a straight line:

$$\bar{\nu}^2 = \left(\frac{37.2}{m/\text{amu}} + 0.54 \right) \times 10^5 \text{ cm}^{-2}. \quad (2)$$

Extrapolating Eq. (2) to ^{16}O , this also very well describes the present assignment of Q at 544 cm^{-1} to O_N in GaN to within a margin of 6%.

V. CONCLUSION

In conclusion we have observed a set of vibrational gap modes in GaN:O near and below the optical phonon band. The mode energies agree well with calculations for substitutional O donors on the N site in an oscillator model. Under hydrostatic pressure the modes shift and change in relative intensity. We associate this behavior with variable screening conditions caused by three different charge states of the impurity. The switching thresholds also coincide with previously observed transitions of the O DX -like center. While higher order defect and complex interactions cannot presently be excluded, the line of evidence strongly supports an assignment of the Q mode at 544 cm^{-1} ($p \approx 0$ GPa) to substitutional O_N in GaN and Q_{1-3} to the corresponding in-basal plane modes in the D^+ , D^0 , and DX^- charge states of the same defect. To our knowledge this is the first identification of a donor vibrational mode in GaN.

ACKNOWLEDGMENTS

The authors thank P. Perlin for advice in the pressure experiment, T. Suski and G. Kaczmarczyk for fruitful discussions, and E. E. Haller and P. Y. Yu for the use of their pressure equipment. This work was supported by JSPS Research for the Future Program in the Area of Atomic Scale Surface and Interface Dynamics under the project of ‘‘Dynamic Process and Control of the Buffer Layer at the Interface in a Highly Mismatched System.’’ Work at Berkeley Lab was performed under the Cooperative Research and Development Agreement with HP Laboratories and supported by the Director, Office of Sciences of the U.S. Department of Energy under Contract No. DE-AC03-76SF00098.

*Electronic address: Wetzels@meijo-u.ac.jp

¹I. Akasaki and H. Amano, Jpn. J. Appl. Phys., Part 1 **36**, 5393 (1997).

²I. Akasaki and C. Wetzels, Proc. IEEE **85**, 1750 (1997).

³I. Akasaki, in *Nitride Semiconductors*, edited by F. A. Ponce, S. P. DenBaars, B. K. Meyer, S. Nakamura, and S. Strite, MRS Symposia Proceedings No. 482 (Materials Research Society, Pittsburgh, 1998), p. 3.

⁴C. Wetzels, T. Suski, J. W. Ager III, E. R. Weber, E. E. Haller, S. Fischer, B. K. Meyer, R. J. Molnar, and P. Perlin, Phys. Rev. Lett. **78**, 3923 (1997).

⁵C. G. Van de Walle, Phys. Rev. B **57**, R2033 (1998).

⁶C. Wetzels and I. Akasaki, in *Properties, Synthesis, Characterization, and Applications of Gallium Nitride and Related Compounds*, edited by J. Edgar, T. S. Strite, I. Akasaki, H. Amano, and C. Wetzels (INSPEC/IEE, London, 1999), p. 284.

- ⁷R. C. Newman, in *Imperfections in III/V Materials*, Semiconductors and Semimetals Vol. 38, edited by E. R. Weber (Academic Press, London, 1993), p. 117.
- ⁸C. Wetzel, W. Walukiewicz, E. E. Haller, J. W. Ager III, I. Grzegory, S. Porowski, and T. Suski, *Phys. Rev. B* **53**, 1322 (1996).
- ⁹T. Suski and P. Perlin, in *Gallium Nitride (GaN)*, Semiconductors and Semimetals Vol. 50, edited by J. I. Pankove and T. D. Moustakas (Academic Press, Boston, 1997).
- ¹⁰W. M. Chen, I. A. Buyanova, M. Wagner, B. Monemar, J. L. Lindstrom, H. Amano, and I. Akasaki, *Phys. Rev. B* **58**, R13 351 (1998).
- ¹¹M. Topf, S. Koynov, S. Fischer, I. Dirnstorfer, W. Kriegseis, W. Burkhardt, and B. K. Meyer, in *III-V Nitrides*, edited by F. A. Ponce, T. D. Moustakas, I. Akasaki, and B. A. Monemar, MRS Symposia Proceedings No. 449 (Materials Research Society, Pittsburgh, 1997), p. 307.
- ¹²I. Grzegory, J. Jun, M. Bockowski, St. Krukowski, M. Wroblewski, B. Lucznik, and S. Porowski, *J. Phys. Chem. Solids* **56**, 639 (1995).
- ¹³C. Wetzel and I. Akasaki, in *Properties, Synthesis, Characterization, and Applications of Gallium Nitride and Related Compounds* (Ref. 6), p. 52.
- ¹⁴C. Wetzel, A. L. Chen, T. Suski, J. W. Ager III, and W. Walukiewicz, *Phys. Status Solidi B* **198**, 243 (1996).
- ¹⁵L. Filippidis, H. Siegle, A. Hoffmann, C. Thomsen, K. Karch, and F. Bechstedt, *Phys. Status Solidi B* **198**, 621 (1996).
- ¹⁶C. Wetzel, H. Amano, I. Akasaki, J. W. Ager III, M. Topf, and B. K. Meyer, *Physica B* **273–274**, 109 (1999).
- ¹⁷A. S. Barker, Jr. and A. J. Sievers, *Rev. Mod. Phys.* **47**, S1 (1975).
- ¹⁸J. M. Zhang, T. Ruf, M. Cardona, O. Ambacher, M. Stutzmann, J.-M. Wagner, and F. Bechstedt, *Phys. Rev. B* **56**, 14 399 (1997).
- ¹⁹T. Mattila and R. M. Nieminen, *Phys. Rev. B* **54**, 1667 (1996).
- ²⁰C. H. Park and D. J. Chadi, *Phys. Rev. B* **55**, 1299 (1997).
- ²¹J. A. Wolk, W. Walukiewicz, M. L. W. Thewalt, and E. E. Haller, *Phys. Rev. Lett.* **68**, 3619 (1992).
- ²²P. Perlin, T. Suski, H. Teisseyre, M. Leszczynski, I. Grzegory, J. Jun, S. Porowski, P. Boguslawski, J. Bernholc, J. C. Chervin, A. Polian, and T. D. Moustakas, *Phys. Rev. Lett.* **75**, 296 (1995).
- ²³E. G. Grosche, R. C. Newman, D. A. Robbie, R. S. Leigh, and M. J. L. Sangster, *Phys. Rev. B* **56**, 15 701 (1997).
- ²⁴P. Perlin, T. Suski, A. Polian, J. C. Chervin, W. Knap, J. Camassel, I. Grzegory, S. Porowski, and J. W. Erickson, in *III-V Nitrides* (Ref. 11), p. 689.